MODELLING THE TOKAMAK EDGE PLASMA WITH A COUPLED 2-D FLUID/MONTE CARLO CODE

H. Gerhauser[1)], H.A. Claaßen[1)], D. Reiter[1,2)]

The 2-d two-fluid code SOLXY /1/ for computing plasma profiles in the edge region of limiter tokamaks has been extended in several directions. First we showed that the poloidal plasma rotation is related to the assumption of an ideally conducting limiter and strongly suppressed in the non-conducting case. Secondly we studied the influence of introducing an anomalous radial viscosity in analogy to the other anomalous perpendicular transport coefficients. Above all we replaced the hitherto purely analytical modelling of the neutral gas transport by a Monte Carlo simulation with the code EIRENE /6/. By application of a "correlation sampling" method the coupled codes rapidly converge towards the self-consistent stationary values of all physical quantities.

We consider the TEXTOR edge plasma in the rectangular integration domain ACFD of Fig. 1 and take $\partial/\partial z \equiv 0$ throughout. We use the full set of Braginskij's two-fluid equations as outlined in /1/. The basic plasma equations for the particle, momentum and energy balances contain the source terms from the recycled neutrals: ($\partial_t = \partial/\partial t$)

$$\partial_t n + \nabla \cdot (n\vec{v}) = S_n \tag{1}$$

$$\partial_t (mn\vec{v}) + \nabla \cdot (mn\vec{v}\vec{v}) = -\nabla p - \nabla \cdot \vec{\pi} + \vec{j} \times \vec{B} + \vec{S}_p \tag{2}$$

$$\partial_t (1.5\, n\, T_e) + \nabla \cdot \vec{Q}_e = \vec{j} \cdot \vec{E} + \vec{v} \cdot (\nabla p_e - \vec{j} \times \vec{B}) + Q_{ei} + W_e \tag{3}$$

$$\partial_t (1.5\, n\, T_i + 0.5\, mn\, \vec{v}^2) + \nabla \cdot \vec{Q}_i = -\vec{v} \cdot (\nabla p_e - \vec{j} \times \vec{B}) - Q_{ei} + W_i \tag{4}$$

We allow for non-ambipolar motion with an electrical current density $\vec{j} = en(\vec{v} - \vec{u})$, where $\vec{v}$ and $\vec{u}$ are the ion and electron velocities. The poloidal component j_z follows from radial equilibrium, the other components are derived from a stream function Ψ and determined by the z-component of (2): ($\partial_x = \partial/\partial x$, $\partial_y = \partial/\partial y$)

$$j_z B = \partial_y p = \partial_y (nT_e + nT_i), \qquad j_x = -\partial_y \Psi, \qquad j_y = \partial_x \Psi \tag{5}$$

$$B\, \partial_x \Psi = -mn\, (v_x \partial_x + v_y \partial_y)\, v_z + S_{pz} - mv_z \tag{6}$$

The term Q_{ei} is the thermal energy exchange between ions and electrons. The electric potential Φ is calculated from the parallel component of the generalized Ohm's law in the limit of infinite conductivities, whereas the radial component yields the poloidal rotation velocity v_z as the sum (finite in general) of the electric and the diamagnetic drift:

$$eE_x = -e\, \partial_x \Phi = -\partial_x p_e / n - 0.71\, \partial_x T_e \tag{7}$$

$$enB\, v_z = en\, \partial_y \Phi + \partial_y p_i \tag{8}$$

The radial diffusion flux $\Gamma^{\perp} = nv_y = -D^{\perp}\, \partial_y n$ is assumed anomalous ($D^{\perp} = 0.6\ m^2/sec$), and the usual time relaxation on the 60×33 numerical grid is restricted to the x-component of (2) and to (1), (3) and (4).

Let us first reconsider the case of a conducting limiter, characterized by a constant potential taken to be zero. Using Bohm's condition $\Gamma^{\parallel} = nv_x = nc_s$ at the limiter, the plasma potential at the plasma side of the Langmuir sheath in front of the limiter is

$$e\Phi = -T_e \ln \left[\sqrt{2\pi m_e (T_e + T_i)/T_e m_i}\ (1 - j_x/enc_s)\right] \sim 3\, T_e \tag{9}$$

with the sound velocity $c_s = \sqrt{(T_e + T_i)/m_i}$. Then integration of (7) from x = L to 0 yields Φ, application of (8) the rotation v_z, and integration of (6) from x=0 to L pro-

1) Institut für Plasmaphysik, Kernforschungsanlage Jülich GmbH, Association EURATOM-KFA, P.O. Box 1913, D-5170 Jülich, FRG.

2) This contribution was sponsored by NET Contract 247/86-9/Fu-D

duces Ψ and j_x, starting with $\Psi(x=0) = 0$. After very few iterations Φ, v_z, Ψ, j_x, j_y are converged. Results are displayed by the plots Pl. 7 to Pl. 9.

In the case of a non-conducting limiter, however, the limiter potential may vary arbitrarily along y. Defining an additional potential $\Phi^*(y)$ and a total potential $\Phi_{nc}(x,y) = \Phi(x,y) + \Phi^*(y)$ with a corresponding $v_{z\,nc}$ from (8) and Ψ_{nc} from (6), Φ^* must be chosen such that $j_{x\,nc} = 0$ at the limiter, which means that the electric current eddies must be closed within the plasma. Hence $\Psi_{nc}(x=L) = 0$, which leads to

$$d^2\Phi^*/dy^2 \int_o^L mn\, v_y\, dx + d\Phi^*/dy \int_o^L m\, S_o\, dx = B^2\, \Psi(L,y) \qquad (10)$$

with S_o originating from S_n and S_{pz}. This differential equation determines $\Phi^*(y)$ if we assume $\Phi^* = d\Phi^*/dy = 0$ for y=0 (no changes far away from the scrape-off layer). Both cases are compared by plots Pl.10 and Pl.11. We find that Φ_{nc} exhibits a monotonic increase from the plasma core to the outer wall instead of a maximum near the separatrix. Furthermore, the rotation $v_{z\,nc}$ and consequently Ψ_{nc} are strongly suppressed.

The dominant components of the viscosity tensor $\bar{\bar{\pi}}$ are taken as

$$\pi_{xx} = -\eta^{\parallel}\, \partial_x v_x, \qquad \pi_{xy} = \pi_{yx} = -\eta^{\perp}\, \partial_y v_x \qquad (11)$$

with $$\eta^{\parallel} = 4\eta_o/3 = 1.28\, n\, T_i\, \tau_i, \qquad \eta^{\perp} = mn\, D^{\perp} \qquad (12)$$

It is consistent to assume that the perpendicular viscosity $\eta^{\perp}$ is also anomalous like the corresponding heat conductivities $\chi_e^{\perp} = \chi_i^{\perp} = nD^{\perp}$. The importance of an anomalous $\eta^{\perp}$ was evidenced by Hutchinson /2/. The viscosities appear in the total heat fluxes:

$$Q_e^{\perp} = 2.5\, n\, T_e\, u_y - \chi_e^{\perp}\, \partial_y T_e \qquad (13)$$

$$Q_i^{\perp} = (2.5\, n\, T_i + 0.5\, mn\, \vec{v}^2)\, v_y - \eta^{\perp}\, v_x\, \partial_y v_x - \chi_i^{\perp}\, \partial_y T_i \qquad (14)$$

$$Q_e^{\parallel} = 2.5\, n\, T_e\, u_x - \chi_e^{\parallel}\, \partial_x T_e - 0.71\, T_e\, j_x/e \qquad (15)$$

$$Q_i^{\parallel} = (2.5\, n\, T_i + 0.5\, mn\, \vec{v}^2)\, v_x - \eta^{\parallel}\, v_x\, \partial_x v_x - \chi_i^{\parallel}\, \partial_x T_i \qquad (16)$$

We prescribe $Q_e^{\perp}$, $Q_i^{\perp}$ at the plasma core boundary (with total particle inflow $\int \Gamma^{\perp} dx = 65 \cdot 10^{19}$/m sec) and require $Q_e^{\parallel} = 5.5\, T_e\, \Gamma^{\parallel}$, $Q_i^{\parallel} = 3.5\, T_i\, \Gamma^{\parallel}$ at the limiter. A typical energy flow diagram is shown by Fig. 2. The η-terms in the parallel equation of motion $-(\nabla\cdot\bar{\bar{\pi}})_x = \partial_x(\eta^{\parallel}\, \partial_x v_x) + \partial_y(\eta^{\perp}\, \partial_y v_x)$ strongly influence the shape of the v_x- and n-profiles, see plots Pl. 1, 2, 12, 13. Near the limiter edge both terms in $(\nabla\cdot\bar{\bar{\pi}})_x$ are of equal order but opposite sign. Thus the presence of an anomalous $\eta^{\perp}$ is essential for reproducing the experimentally observed steepening of the toroidal and radial profiles when approaching the limiter edge. Even with inclusion of $\eta^{\perp}$ we must choose $\eta^{\parallel}$ smaller than classical in order to avoid too much flattening of the profiles (Pl. 13). We take $0.22\, \eta^{\parallel}_{class}$ and use the same factor 0.22 also for $\chi_e^{\parallel}$ and $\chi_i^{\parallel}$, because all parallel coefficients vary $\sim T^{5/2}$. Note that the proposed reduction with respect to classical values is suggested also by Igitkhanov /3/ from non-local effects on the distribution function and from collisions with impurities.

For the recycling of neutrals at the limiter and their interaction with the s.o.l. plasma we use and compare two models, a Monte Carlo simulation as implemented in the code EIRENE /6/, and an analytic approximation /1/. The D^+-ions impinging on the limiter are nearly monoenergetic with near-normal incidence due to the acceleration in the Langmuir sheath: $E_i = \overline{E_i} = Q_i^{\parallel}/\Gamma^{\parallel} + e\,\Phi \approx 3.5\, T_i + 3\, T_e$ and $\Gamma^{\parallel} = \int\int \gamma(E_i,\Omega_i)\, dE_i d\Omega_i$. The flux distribution γ at the limiter is simulated consistently with the shifted Max-

wellian ion distribution function entering into the derivation /1/ of the boundary conditions for the plasma equations. Part of the neutralized D^+ are reflected as "fast" neutrals with reduced energy and $\Gamma_o^f = -R_N\Gamma^{\|} = -\int\int\int\int \gamma(E_i,\Omega_i)\, R(E_i,\Omega_i,E,\Omega)\, dE_i d\Omega_i dE d\Omega$, the rest is released as D_2-molecules and treated as "slow" Frank-Condon atoms with energy $E_o^s = 5$ eV and $\Gamma_o^s = -\Gamma^{\|} - \Gamma_o^f$. We choose the reflexion kernel R as described in /5/ for limiter and wall, but admit only a narrow cos-like angular distribution ($\alpha \lesssim 5.4\ ^o$) of the source neutrals close to the limiter normal. Many individual Monte Carlo trajectories are followed until ionization or loss across the plasma core boundary. Higher charge exchange generations are all included and added to the fast component. Neutrals hitting the wall or limiter experience loss of energy and non-specular reflexion.

In the analytic model all incident ions have $E_i = \overline{E_i}$ and $\alpha_i = 0$, the energy distribution $J(E) = R(E_i,E)$ is averaged such that the mean energy E_o^f is attributed to all fast neutrals, and the reflexion coefficients $R_N = \int J(E)\, dE$ and R_E are approximated by

$$\frac{E_o^f}{E_i} = \frac{R_E}{R_N} = \frac{\int E\, J(E)\, dE}{E_i \int J(E)\, dE} = \frac{0.813 - 0.286 \log_{10}(0.4\, E_i)}{0.962 - 0.259 \log_{10}(0.4\, E_i)} \qquad (17)$$

Emission is discrete into 17 distinct directions, and the 17 fast and slow beams are exponentially damped by electron impact ionization and charge exchange according to $n_o^{f,s} \sim \exp[-\int ds\, (\nu_I + \nu_{cx}) / v_o^{f,s}]$ with the frequencies ν_I and ν_{cx} and the velocities $v_o^{f,s} = \sqrt{2\, E_o^{f,s}/m}$. Reflexion at the wall is elastic and specular, cx-neutrals count as lost. For both models the source terms in (1) to (4) are calculated as follows (with s and f to be summed, e.g. $n_o = n_o^f + n_o^s$) :

$$S_n = \nu_I\, n_o = n\, S_I(T_e)\, n_o \qquad (18)$$

$$S_{px,z} = \nu_I\, m\, \Gamma_{ox,z} + \nu_{cx}\, m\, (\Gamma_{ox,z} - n_o v_{x,z}) \qquad (19)$$

$$W_e = -\nu_I\, n_o\, E_I - \nu_*\, n_o\, E_* \qquad (20)$$

$$W_i = \nu_I\, \varepsilon_o + \nu_{cx}\, n_o\, (E_{ocx} - 0.5\, m\, \vec{v}^2 - 1.5\, T_i) \qquad (21)$$

with $\nu_{cx} = n\, S_{cx}(T_{ieff})$, $T_{ieff} = T_i + \pi\, (0.5\, m\, \vec{v}^2 + E_{ocx})/4$ (22)

Here Γ_o and ε_o are the neutral flux and energy densities, S_I and S_{cx} the rate coefficients of Janev /4/, $E_I = 13.6$ eV and $E_* = 10.2$ eV the ionization and excitation energies. The Monte Carlo code is able to estimate "responses" $\langle g \rangle = \int g(\vec{v}_o)\, f(\vec{v}_o)\, d\vec{v}_o$ for arbitrary detector functions g. Special cases are $\langle 1 \rangle = n_o$, $\langle 0.5\, m\, \vec{v}_o^2 \rangle = \varepsilon_o$, etc. This allows us to distinguish carefully between the mean energy $E_o = \varepsilon_o / n_o$ of all neutrals and the mean energy $E_{ocx} = \langle 0.5\, m\, \vec{v}_o^2 \cdot \nu_{cx}(\vec{v}_o) \rangle / \langle \nu_{cx}(\vec{v}_o) \rangle$ of those neutrals that undergo a cx reaction, $E_{ocx}^f > E_o^f$, since higher energies are more probably affected by cx. Only for slow neutrals $E_{ocx}^s = E_o^s = 5$ eV. Using a tracklength estimator technique for all "responses" without any non-analogous methods, the history of 30 000 particles requires about 3 min of CPU-time on a Cray X-MP, resulting in statistical errors of ≈ 1 % for the averaged neutral densities. We couple the 2-d fluid code SOLXY with the Monte Carlo code EIRENE and iterate the plasma and neutral gas parameters by running both codes alternately. An essential improvement towards a successful coupling is the application of "correlation sampling". This means that, by an appropriate modification of the sequence of random numbers, the particle trajectories of two successive runs of EIRENE are positively correlated such that for small changes in the background plasma they also suffer only small variations: the stochastic fluctuations are "frozen". Under

these conditions the iteration converges rapidly towards the self-consistent stationary values of all physical quantities. The convergence is further improved by updating the source terms (18) to (21) every 20 time steps with the changed plasma parameters n, $\vec{v}$, T_e, T_i and with rescaled n_o, Γ_o, ε_o according to the change in the total flux Γ_{oR} of limiter recycled neutrals. We find strongly damped oscillations for all plasma variables and global neutral quantities, shown in Fig. 3 for Γ_{oR} and for the total energy transfer $\Delta E_{cx} = \iint W_{icx}\, dxdy$ from neutrals to ions by cx-reactions. After only 5 iterations the convergence is excellent. There remain small fluctuations in local neutral quantities like n_{omax}, but due to the positive correlation the relative changes in the iterated values are far below the relative standard deviations (some o/oo compared to some %). However, if correlation sampling is switched off (iterations 6 to 10), the global quantities begin to oscillate again, and the local n_{omax} is subject to greatly enhanced fluctuations. The n_o-profiles are displayed by Pl.6 for Monte Carlo and by Pl.5 for the analytic beams (same plasma background). The changes in the self-consistently converged plasma parameters after passing from the analytic to the Monte Carlo model are ≈ 2 % for n, v_x, T_e, T_i and ≈ 5 % for Φ, v_z, Ψ. We conclude that the s.o.l. plasma is remarkably insensitive to the approximations in the analytic neutral gas model. EIRENE admits future refinements with larger emission angles and D_2-molecules.

/1/ H. Gerhauser, H.A. Claaßen, Report JÜL-2125, KFA Jülich, May 1987
/2/ I.H. Hutchinson, Ion Collection by Probes ...., Report MIT/PFC/JA-87-44, Nov. 1987
/3/ Yu. L. Igitkhanov et al., Papers a08 and a29, this conference
/4/ R.K. Janev et al., Atomic and Molecular Processes ...., Report PPPL-TM-368, 1985
/5/ A. Nicolai and D. Reiter, J. of Computational Physics 55, 129 (1984)
/6/ D. Reiter, Report JÜL-1947, KFA Jülich, August 1984

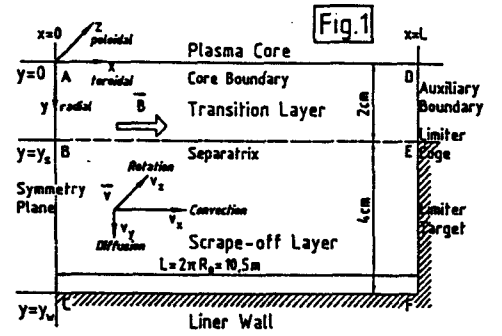

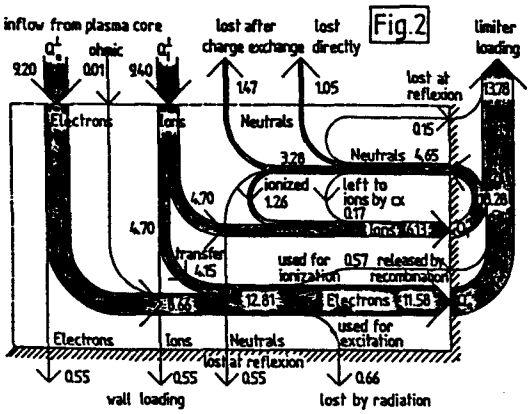

Fig.1: Geometry of Boundary Layer
Fig.2: Energy Flow Diagram [kW/m]
Fig.3: Convergence of Coupled Fluid/Monte-Carlo Code

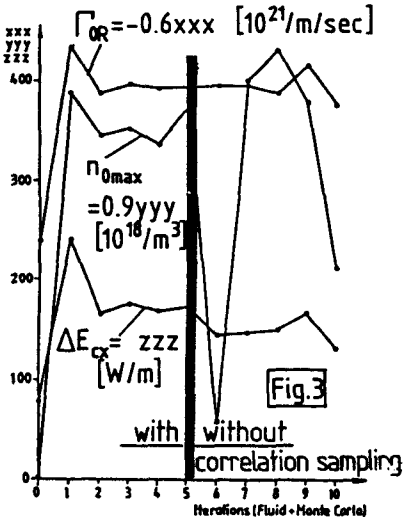

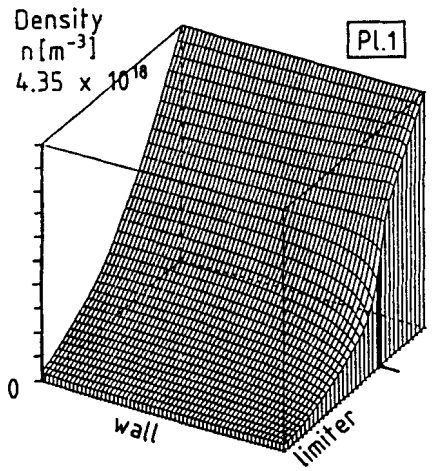
Density
n[m⁻³]
4.35 x 10¹⁸
Pl.1
0
wall
limiter

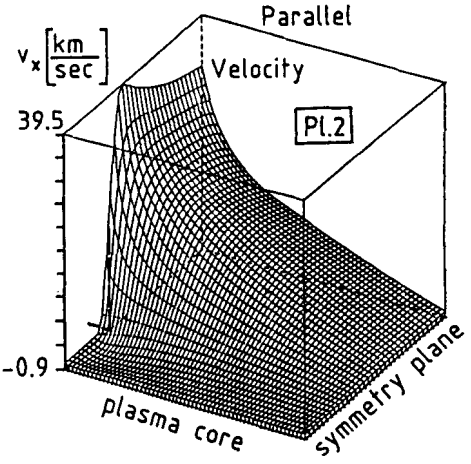
Parallel
Velocity
v_x [km/sec]
39.5
Pl.2
-0.9
plasma core
symmetry plane

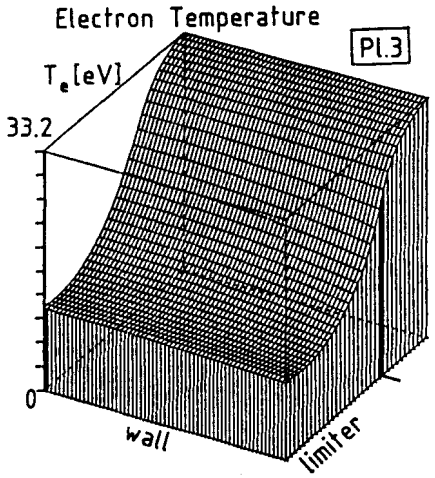
Electron Temperature
T_e[eV]
33.2
Pl.3
0
wall
limiter

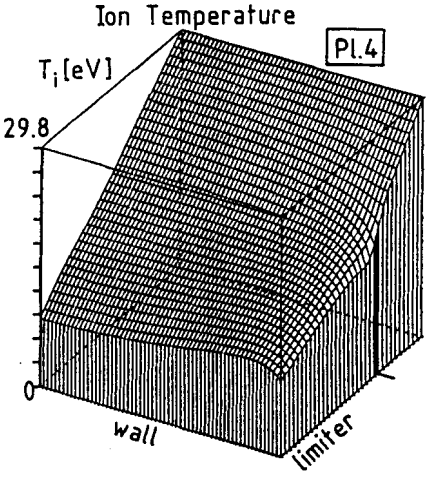
Ion Temperature
T_i[eV]
29.8
Pl.4
0
wall
limiter

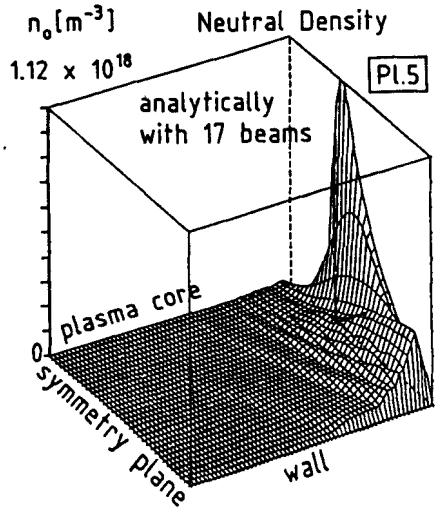
n_o[m⁻³]
Neutral Density
1.12 x 10¹⁸
Pl.5
analytically
with 17 beams
plasma core
0
symmetry plane
wall

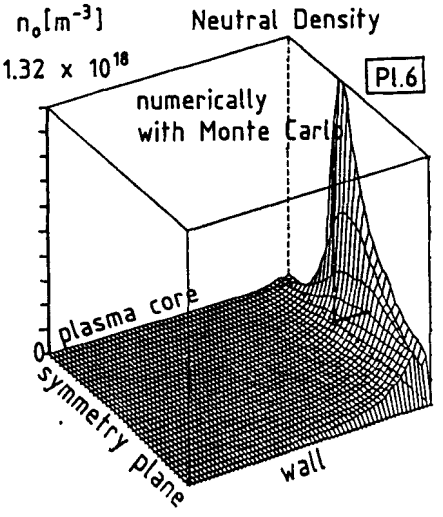
n_o[m⁻³]
Neutral Density
1.32 x 10¹⁸
Pl.6
numerically
with Monte Carlo
plasma core
0
symmetry plane
wall

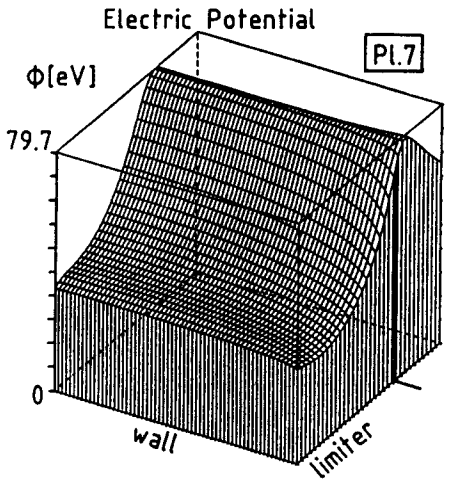
Electric Potential
Pl.7
Φ[eV]
79.7
0
wall
limiter

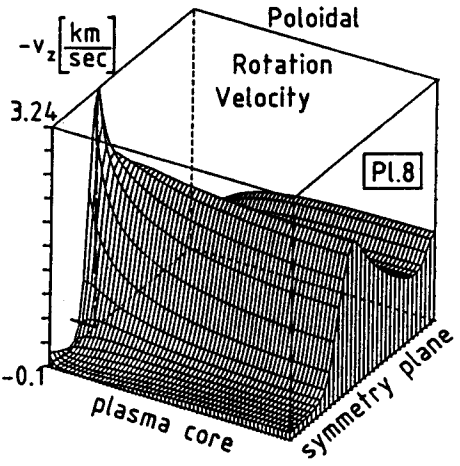
Poloidal
Rotation
Velocity
Pl.8
$-v_z\left[\frac{km}{sec}\right]$
3.24
-0.1
plasma core
symmetry plane

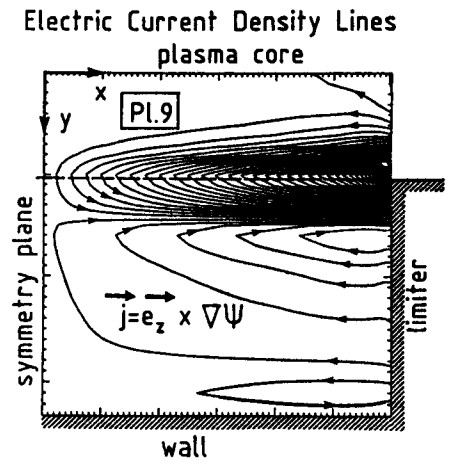
Electric Current Density Lines
plasma core
Pl.9
x
y
symmetry plane
$\vec{j}=\vec{e}_z \times \nabla\Psi$
limiter
wall

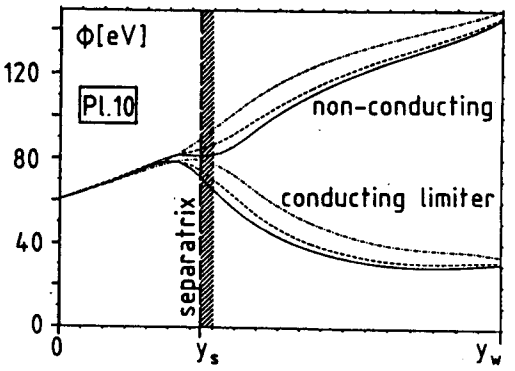
Φ[eV]
Pl.10
120
80
40
0
non-conducting
conducting limiter
separatrix
y_s
y_w

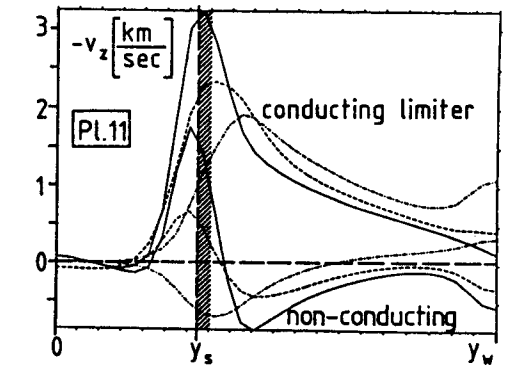
$-v_z\left[\frac{km}{sec}\right]$
Pl.11
3
2
1
0
conducting limiter
non-conducting
y_s
y_w

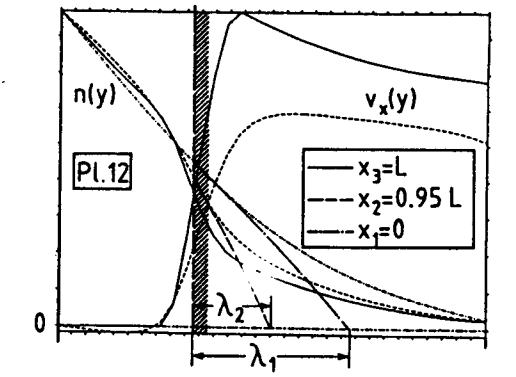
n(y)
$v_x(y)$
Pl.12
$x_3=L$
$x_2=0.95\,L$
$x_1=0$
0
λ_2
λ_1

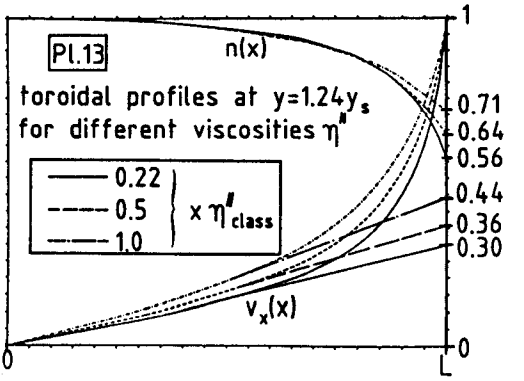
Pl.13
n(x)
toroidal profiles at $y=1.24y_s$
for different viscosities η''
0.22
0.5
1.0
$\times\,\eta''_{class}$
$v_x(x)$
1
0.71
0.64
0.56
0.44
0.36
0.30
0
L